

## Characterization of glass surfaces by X-ray reflectivity<sup>1)</sup>

Olaf Anderson and Klaus Bange  
Schott Glaswerke, Mainz (Germany)

---

Surfaces of soda-lime and borosilicate glasses produced by the float technique as well as polished BK-7, fused silica and aluminosilicate glasses are investigated by means of grazing incidence X-ray reflectometry. Thin layers are found at all surfaces with properties which differ significantly from the bulk properties of the respective material. Fused silica surfaces exhibit a hydrated layer with a thickness of approximately 17 nm and a slightly reduced density. A thin leached layer with a density of approximately  $2 \text{ g} \cdot \text{cm}^{-3}$  is analyzed on BK-7 glass. A variation in the rms roughness between 0.7 and 1.5 nm is found for aluminosilicate glasses depending on the polishing procedure. Pronounced differences are obtained between the air and the tin bath side of soda-lime float glass, whereas for borosilicate float glass only small differences in density between the two sides of the glass are measurable. The evolution of the initial stages of corrosion is demonstrated on soda-lime glass in dependence on the storage time.

### Charakterisierung von Glasoberflächen mittels Röntgen-Reflektometrie

Oberflächen von Kalk-Natron- und Borosilicat-Floatglas sowie polierte Oberflächen von BK-7-, Kiesel- und Aluminosilicatglas wurden mittels Grazing Incidence X-ray Reflectometry charakterisiert. Auf Kieselglasoberflächen wird eine etwa 17 nm dicke Schicht mit geringfügig reduzierter Dichte gefunden. BK-7-Glasoberflächen besitzen eine dünne Auslaugschicht mit einer Dichte von rund  $2 \text{ g} \cdot \text{cm}^{-3}$ . In Abhängigkeit vom Polierverfahren werden rms-Rauhigkeiten auf Aluminosilicatglasoberflächen von 0,7 bis 1,5 nm gemessen. Markante Unterschiede zwischen Gas- und Zinnbadseite werden bei Kalk-Natron-Floatgläsern gefunden, während für Borosilicat-Floatglas nur geringe Unterschiede zwischen den beiden Glasseiten gemessen werden. Die Entwicklung der Anfangsstadien von Glaskorrosion in Abhängigkeit von der Lagerzeit wird für Kalk-Natronglas demonstriert.

## 1. Introduction

Various properties of glass surfaces possess an increasing significance for the commercialization of products and their technological importance rises, in particular for special applications, i.e. the nature of the surface and the modification during different processes are of considerable interest for manufacturers and users of the glasses. Numerous chemical and mechanical reactions occur on the surface during the production process, e.g. floating, drawing, pressing, polishing, cleaning, storing in different media, during pretreatment before coating or during the product lifetime. Therefore, glass surfaces represent a wide area of research today, especially that on the stability of the surfaces exposed to different environments during fabrication, processing, storing or application. Today, it is known that many of the so-called "glass problems" are, in reality, surface problems and, in general, that glass surface reactions depend on the composition of the glasses, the heating or cooling procedure, on the reacting agents of surrounding atmosphere, the composition and pH values of the solution and on the temperature and time of the reactions [1].

The whole spectrum of surface-analytical tools has been applied to glass surfaces [2 and 3]. A number of

these techniques are hampered by charging problems or matrix effects when electrons or ions are used as probes. Also, various artifacts may be created, e.g. changes of the composition by preferential sputtering, charge-induced diffusion of glass elements or desorption phenomena occurring under vacuum limit the accessible information. Although high-resolution microscopy such as Atomic Force Microscopy (AFM), which operates in air, provides useful information about changes on glass surfaces such as topography on nanometer scale, it cannot look below the surface, where the initial stages of corrosion or leaching take place.

The present paper describes investigations of the roughness, the density and the thickness of altered surface layers on different glasses evoked by different manufacturing processes. Grazing Incidence X-ray Reflectometry (GIXR) is used to study the surfaces of soda-lime and borosilicate glasses obtained from float processes, the corrosion of soda-lime float glass, and the polishing process of BK-7 and aluminosilicate glasses. All materials exhibit a modified surface region which can be expressed in differences in density.

## 2. Experimental

At grazing incidence all X-ray techniques become surface-sensitive, because below the angle of total reflection the X-rays penetrate only 2 to 7 nm into condensed mat-

---

Received January 30, 1997.

<sup>1)</sup> Presented in German at: 70th Annual Meeting of the German Society of Glass Technology (DGG) on June 4, 1996 in Cottbus (Germany).

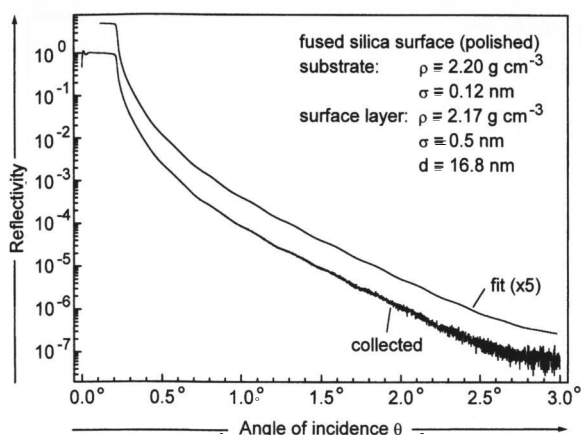


Figure 1. Reflectivity of a polished fused silica surface versus angle of incidence  $\theta$ . The weak oscillations are caused by a thin surface layer with slightly lower density.

ter [4]. Therefore, it turns out that GIXR is the right technique to match the demands for thin layers on glass surfaces and their interfaces. The reflection of X-rays at flat surfaces follows the classical optical principles of refraction and reflection by Snell's law with optical indices related to the used wavelength and to the medium properties. In the hard X-ray range the index of refraction,  $n$ , is slightly smaller than one and a complex number [5]. It can be written as

$$n = 1 - \delta + i\beta,$$

where  $\delta$  and  $\beta$  are positive quantities and of the order  $10^{-5}$  to  $10^{-6}$ . The absorptive correction

$$\beta = \mu \lambda / 4\pi$$

is proportional to the coefficient of linear absorption,  $\mu$ , and the photon wavelength,  $\lambda$ . The dispersive correction,  $\delta$ , is proportional to  $\lambda^2$ , to the mass density,  $\rho$ , and the real part,  $(Z + f')$ , of the atomic form factor. Since  $n$  is smaller than one ( $1 - \delta$ ), the beam is refracted away from the surface normal when it enters into the matter. Therefore, there exists a critical angle,  $\theta_{1c}$ , for the incident beam at which the angle of the refracted beam  $\theta_2 = 0$ . Below  $\theta_{1c}$  the beam is totally reflected. When absorption can be neglected, this occurs at  $\theta_{1c} = \sqrt{2\delta_2}$ . In the hard X-ray range this angle is below  $0.5^\circ$  for most materials. The determination of the critical angle gives the mass density of the reflected medium. In reality, however,  $\theta_{1c}$  cannot be determined in a simple way from the reflectivity, because the drop in reflectivity at the critical angle is smeared out by absorption and by surface roughness. The latter is taken into account by an exponential Debye-Waller-type factor to the Fresnel reflectivity derived from the model of Névet and Croce [6]. For more details on X-ray reflectivity see [4 and 7].

The information which can be extracted from the reflectivity versus angle of incidence curves includes the density,  $\rho$ , of the substrate and of the thin surface layers,

the thickness of the layers,  $d$ , and the interface roughnesses,  $\sigma$ . This information is extracted by fitting the experimental data with the program GIXA (Philips Analytical X-ray, Almelo (The Netherlands)), which is based on the transfer matrix method [8] and uses the simplex algorithm in combination with simulated thermal annealing [9]. The accuracy of the results depends on the quality of the sample and on the accuracy with which the angle of incidence is determined. Flat substrates such as float glass are well suited. The accuracy for the determination of the density is proved to be within  $\pm 1\%$ . The thickness of surface layers can be determined within  $\pm 0.1$  nm. The root mean square (rms) values of the interfaces are reproducible within  $\pm 3\%$ .

The measurements are performed by an instrument based on a standard Philips diffractometer (Philips, Eindhoven (The Netherlands)) with a PW1830 generator and an optically encoded PW3020 goniometer (using a step size between  $0.004^\circ$  and  $0.001^\circ$  in  $\theta$ ). The X-ray source is a sealed tube with copper anode and long-fine focus of height  $40 \mu\text{m}$ . A  $1/32^\circ$  divergence slit and two parallel receiving slits of  $100 \mu\text{m}$  are used in a parallel beam configuration. A graphite monochromator is placed before a gas proportional counter. The direct beam intensity at  $40 \text{ kV}/40 \text{ mA}$  reaches  $1.5 \cdot 10^7$  cps. Since the dynamic range of the X-ray detector is limited to  $5 \cdot 10^5$  cps (= counts per second) for reflectivity curves, an extenuator (nickel foil, factor 235) is used at high intensities, which increases the dynamic range by 7 to 8 decades. The underground counting rate is typically 0.3 to 0.6 cps. The sample stage is motorized and allows the adjustment of the sample in the direct beam with an accuracy in height of  $1 \mu\text{m}$  and a tilt angle of  $0.01^\circ$ . The precise adjustment of the incident and reflected beam with an accuracy of better than 1 arc second is done just below the critical angle by "rocking-curve-type" measurements.

The samples of the polished glasses (fused silica, BK-7, aluminosilicate) have diameters of about 50 mm and thicknesses between 2 and 4 mm. The polishing is performed at Deutsche Spezialglas AG (DESAG, Grünenplan (Germany)) by standard procedures down to an rms roughness of about 1 nm and controlled by interferometric microscopy TOPO-3D (WYKO Corp., Tucson, AZ (USA)). For the experiments on float glass specimens of commercial soda-lime glass and borosilicate glass from Jenaer Glaswerk GmbH, Jena (Germany), with a thickness of 4 mm are used. Tin bath (bottom) and air (top) side of the glasses are cleaned by a typical industrial cleaning procedure, which is described in detail elsewhere [10]. For the corrosion experiment fresh soda-lime float glass from Flachglas AG, Gelsenkirchen (Germany), is used and stored at a temperature of  $40^\circ\text{C}$  and at 95% relative humidity.

### 3. Results and discussion

Figure 1 illustrates the bearing of the hydration process on the reflectivity of a fused silica surface evoked by the

polishing and cleaning procedure. The material is used as an example of an amorphous oxide glass which is often applied as substrate for coatings. Before coating the surface has to be polished and cleaned carefully. No components of the  $\text{SiO}_2$  matrix are leached out by these procedures as in other glasses. Only some hydrogen ions from hydrous solutions are able to diffuse into the silica where hydroxyl groups will be formed [11]. This process of the hydration of a thin surface layer on silica can be detected by GIXR.

Figure 1 shows the reflectivity versus the angle of incidence of a polished fused silica surface. Below the critical angle,  $\theta_c$ , of about  $0.22^\circ$  total reflection takes place and the reflectivity is nearly one. With increasing angle of incidence the reflectivity decreases as expected, but a weak oscillation is also noticeable in the curve. This is a strong indication of a thin surface layer with deviating density. The simulation of the measurement, which is displaced by a factor of 5 in figure 1 for clearance, is calculated with a model which includes a thin layer on top of the unchanged bulk material and describes the measured curve exactly. A density of  $2.17 \text{ g} \cdot \text{cm}^{-3}$  (in comparison to  $2.20 \text{ g} \cdot \text{cm}^{-3}$  for the bulk) and a thickness of 16.8 nm are calculated (figure 1) for the surface layer. The rms value of 0.5 nm for the roughness of the sample surface is in accordance with the high quality of the polishing. An rms value of only 0.12 nm is obtained for the interface between the hydrated surface layer and the bulk material. This indicates that the hydrated layer is nearly homogeneous and only a weak density gradient may be present. The obtained results suggest that the interaction of hydrogen-containing species weakens the bonding in the surface layer, which leads to enlarged interatomic distances and a decreased density [11].

The leaching of optical glasses like BK-7 by polishing and cleaning of the surfaces is apparent in the reflectivity data shown in figure 2. The measured data (dotted) of the reflectivity from a polished BK-7 glass surface is compared with two curves obtained from the simulation with two different models. One model considers only the glass surface without a leached layer (dashed curve), and the other model uses a thin leached layer on the surface (solid curve). It is obvious that the measured data can be described only in the second case under the assumption of a thin surface layer. The results of the accurate simulation are summarized in table 1. Usually, leached layers on glass surfaces are not homogeneous and possess gradients in density [12 to 14]. These cannot be described by the simulation program exactly, i.e., a model with different thin homogeneous layers has to be used for approximation. In the case that only one layer is assumed the presence of a density gradient becomes apparent by a higher value for the roughness of the interface between the (leached) layer and the bulk material and, sometimes, for the surface. For the BK-7 glass (table 1) the high rms roughness of 1.5 nm for the interface and the relatively high rms value

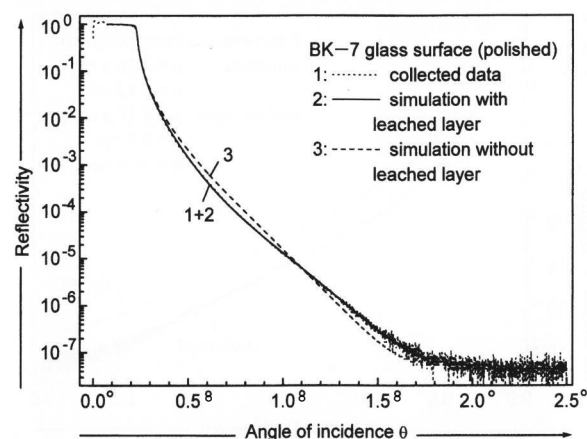


Figure 2. Reflectivity of a polished BK-7 glass surface versus angle of incidence  $\theta$ . The measured data can only be described with a simulation which includes a thin leached surface layer (see text).

Table 1. Results of the simulation of the reflectivity of a polished BK-7 glass surface

	density in $\text{g} \cdot \text{cm}^{-3}$	roughness in nm	thickness in nm
BK-7 glass	2.52	1.5	=
leached layer	$\approx 2.0$	1.0	2.4

for the surface indicate that a pronounced gradient in density exists. This can be verified easily by depth profile analysis [13]. For thin layers with gradients in density the value for the thickness represents only the corresponding value for a homogeneous layer with the same effect on the reflectivity curve. It is known that during the leaching of BK-7 glass an interdiffusion between barium and potassium (but not sodium) and hydrogen takes place, which reduces the density in a thin leached surface layer drastically. The thickness of the leached layer with reduced density can be limited to a few nanometres (as in the present case) if suitable and optimized procedures for polishing and cleaning are used. Otherwise, leached layers with a thickness of a few hundreds of nanometre may be formed [14].

The quality of polishing, i.e. the roughness, of glass surfaces can be determined very accurately by reflectometry measurements. An example for an aluminosilicate glass is shown in figure 3, which demonstrates the influence of surface roughness on the shape of the reflectivity curve. The decrease in reflectivity with increasing angle of incidence is a direct function of the surface roughness and corresponds with the theory [4 and 6]. Even very small changes in the rms roughness can be detected reproducibly. Moreover, figure 3 demonstrates the temporal improvement of the quality of a special polishing process recently established. In the range of incidence angle from  $0.8^\circ$  to  $2.5^\circ$  the reflectivity of the sample surface is directly correlated with the roughness.

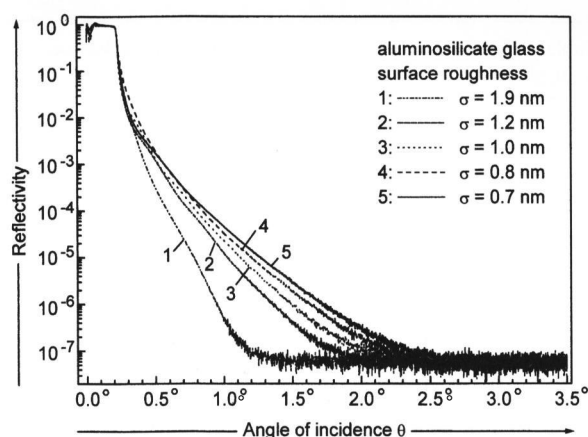


Figure 3. Reflectivity of polished surfaces of an aluminosilicate glass versus angle of incidence  $\theta$ . The influence of the surface roughness (rms value  $\sigma$ ) on the shape of the curves is obvious. With increasing roughness the reflectivity of the surface decreases significantly.

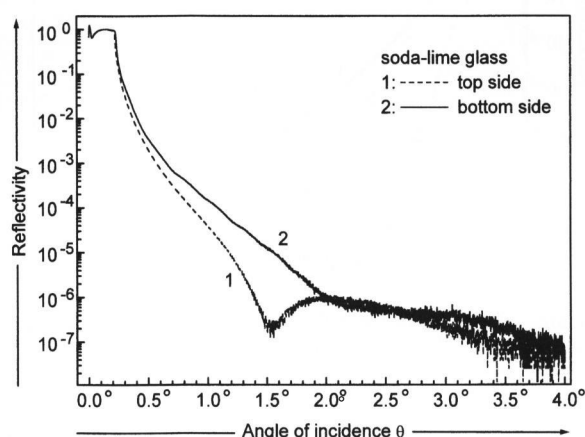


Figure 4. Reflectivity of both sides of soda-lime float glass versus angle of incidence  $\theta$ . The tin content on the bottom side of the glass causes a higher reflectivity and weak oscillations.

Table 2. Fit parameter for the reflectivity data of soda-lime float glass

		top side	bottom side
bulk glass	$\rho$ in $\text{g} \cdot \text{cm}^{-3}$	2.48	2.52
	$\sigma$ in nm	0.6	0.4
leached layer	$\rho$ in $\text{g} \cdot \text{cm}^{-3}$	2.38	2.55
	$d$ in nm	2.7	14.3
	$\sigma$ in nm	0.3	0.2
gel layer	$\rho$ in $\text{g} \cdot \text{cm}^{-3}$	1.42	1.85
	$d$ in nm	1.4	1.0
	$\sigma$ in nm	0.4	0.3

With increasing roughness the amount of diffusely scattered X-rays increases and therefore, the intensity of the specular-reflected X-rays decreases. The apparently

unsystematic shape of the curves in figure 3 in the low angle range of  $0.25^\circ$  to  $0.6^\circ$  is not directly induced by roughness. These parts of the data are dominated by the variations in the leached layers which are caused by the polishing and cleaning processes.

Figure 4 shows typical reflectivity curves of both sides of soda-lime float glass together with their best fits (simulation). The shape of reflectivity curves from the bottom and top side of soda-lime float glass differs drastically from each other. Two surface layers have to be assumed in order to describe the data in a satisfactory way. The need for a second layer with low density is seen in the experimental data by the pronounced minimum at about  $1.5^\circ$  for the top side and the structure between  $2^\circ$  and  $3.5^\circ$  for the bottom side. The results of the fits are summarized in table 2. The first surface layer at the top side (leached layer) has a density ( $2.38 \text{ g} \cdot \text{cm}^{-3}$ ) considerably smaller than the bulk glass ( $2.48 \text{ g} \cdot \text{cm}^{-3}$ ). On the bottom side a density of  $2.52 \text{ g} \cdot \text{cm}^{-3}$  is found. Here the surface layer is thicker (14.3 nm) and possesses a density of  $2.55 \text{ g} \cdot \text{cm}^{-3}$ , which causes oscillations in the experimental data between  $1^\circ$  and  $2^\circ$ .

Flat soda-lime glasses are industrially produced on a large scale by the continuous float process, today's predominant process for flat glasses. Here the bottom surface of the glass ribbon remains in direct contact with molten tin for several minutes. Tin from the float bath diffuses into the bottom side of the glass ribbon, whereas sodium is transferred from the glass melt to the metal phase [15]. In addition, chemical reactions with the atmosphere take place, e.g. during transport and cooling of the glass ribbon or during cleaning. The differences in the properties of the two sides of the glass plates, which are induced by the float process, are preserved until the glass is coated. The reason for the higher density at the bottom side is the well known diffusion of tin into the glass surface and the enrichment of iron in this surface [7 and 15]. In addition, a very thin surface layer with a low density is found on both sides which causes the unusual shape of the curves at higher angles of incidence. This layer is attributed to a gel layer which is formed at the glass surface by the cleaning procedure. The layer on the top side of the float glass always reveals a lower density than on the bottom side.

In a recently published paper [16], reflectivity data were shown which differ significantly from the data shown above. The reason can be found in the different cleaning procedures for the analyzed samples. In the cited paper, the float glass samples are washed in water and rinsed with deionized water. Commonly it is known that float glass has to be cleaned by stronger and more effective procedures in industrial cleaning machines [10] to remove sulfates, carbonates and tin particles from the glass surfaces. This is especially important for glasses which will be coated by antireflecting layers. These industrial cleaning procedures produce special surface properties like leached layers and gel layers on glasses. Therefore, the data shown in [16] are not representative



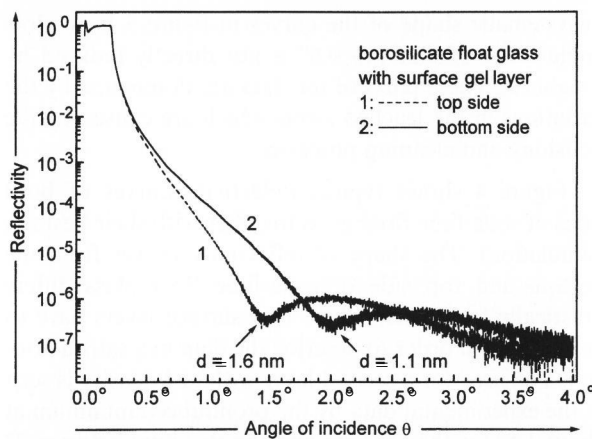


Figure 5. Reflectivity of both sides of borosilicate float glass versus angle of incidence  $\theta$ . The shapes of the curves are comparable and differ only due to the thickness of the thin gel layer on the glass surface.

for float glass used in industrial coating production. When surfaces of float glass are cleaned with a process using HF the differences between top and bottom side of the glass vanish, because the enrichment of tin and iron in the surface is removed. In this case, no gel layer is found [10].

The experimental data of borosilicate float glass are shown in figure 5 and the results of the fitting procedures are summarized in table 3. No influence of tin on the density of the bottom side can be detected for borosilicate glass. On both sides, a density for the bulk glass of  $2.23 \text{ g} \cdot \text{cm}^{-3}$  is determined. A 4.6 nm thick leached surface layer with a slightly lower density ( $2.21 \text{ g} \cdot \text{cm}^{-3}$ ) has to be assumed at the bottom side. A very thin gel layer is found on both sides. The difference in the thickness of this layer between top and bottom side is obvious in the experimental data from the position of the remarkable minimum in the curves at  $1.5^\circ$  and  $2^\circ$ , respectively.

The reason for the different behaviour of soda-lime and borosilicate float glass is the chemical resistivity of borosilicate float glass to leaching and corrosion. During the float process the diffusion of tin into the bottom side of borosilicate glass and the outdiffusion of sodium into the molten tin are much weaker in comparison to soda-lime glass [10 and 15]. Therefore, both sides of borosilicate float glass exhibit nearly the same behaviour. Moreover, its chemical resistivity leads to a much weaker influence of leaching and corrosion during cleaning and storage.

X-ray reflectivity curves of the top side of soda-lime float glass are depicted in figure 6 for different storage times. The reflectivity of a fresh new surface is compared with data obtained after storing at a temperature of  $40^\circ\text{C}$  and at 95% relative humidity. The data were taken after cleaning of the glasses. The reflectivity of the fresh new surface exhibits a nearly uniform shape and differs from the respective curve in figure 4, because this glass

Table 3. Fit parameter for the reflectivity data of borosilicate float glass

		top side	bottom side
bulk glass	$\rho$ in $\text{g} \cdot \text{cm}^{-3}$	2.23	2.23
	$\sigma$ in nm	0.2	0.3
leached layer	$\rho$ in $\text{g} \cdot \text{cm}^{-3}$	—	2.21
	$d$ in nm	—	4.6
	$\sigma$ in nm	—	0.3
gel layer	$\rho$ in $\text{g} \cdot \text{cm}^{-3}$	1.7	1.6
	$d$ in nm	1.6	1.1
	$\sigma$ in nm	0.5	0.3

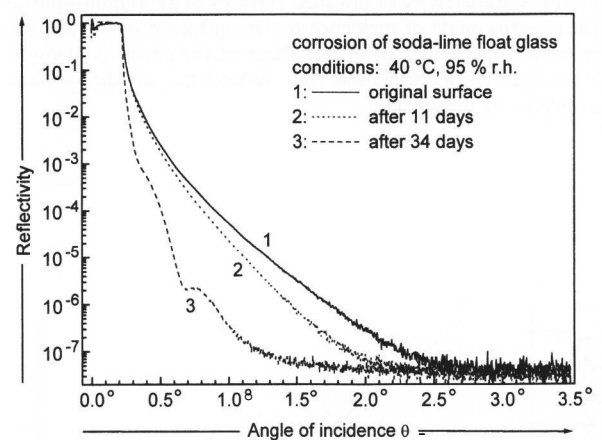


Figure 6. Changes in the reflectivity of the top side of soda-lime float glass due to corrosion of the surface during storage at  $40^\circ\text{C}$  and 95% relative humidity.

has been stored for some days under ambient conditions. Already after 11 d of storage under humid conditions the reflectivity of the surface decreases significantly. A storage of 34 d decreases the reflectivity drastically and an oscillation of the curve becomes visible. All three curves can be fitted well by a simple model including a leached layer with reduced density and/or a gel layer. The results of the simulations are summarized in table 4.

During the storage of glasses under ambient atmospheric conditions the surface properties change. The reasons can be the hydration of a surface layer by atmospheric moisture, the adsorption of water including carbonates onto the surface and corrosion. These changes are accelerated by humid conditions and a higher temperature as in the present case. Due to leaching and corrosion gradients in density are formed, which is recognizable from the relatively high values for the rms roughness of the interfaces. Therefore, the values for the density of the layers in table 4 are only a kind of mean values and the layer thicknesses should not be regarded as absolute values. The reflectivity of the original surface can be described by introducing a thin leached layer with reduced density and a roughness of 0.6 nm which is caused by the preceding cleaning procedure.

Table 4. Fit parameter obtained by simulation for the top side of soda-lime float glass after storage at 40 °C and 95% relative humidity for different times

		original	after 11 d	after 34 d
bulk glass	$\rho$ in $\text{g} \cdot \text{cm}^{-3}$	2.48	2.48	2.48
	$\sigma$ in nm	0.9	1.1	0.9
leached layer	$\rho$ in $\text{g} \cdot \text{cm}^{-3}$	2.0	–	2.2
	$d$ in nm	0.9	–	1.1
	$\sigma$ in nm	0.6	–	3.7
gel layer	$\rho$ in $\text{g} \cdot \text{cm}^{-3}$	–	1.2	1.2
	$d$ in nm	–	0.7	8.8
	$\sigma$ in nm	–	0.7	2.5

After a storage of 11 d the beginning of the corrosion process leads to a lower reflectivity, which can be described by a thin gel layer with a density of about  $1.2 \text{ g} \cdot \text{cm}^{-3}$ . Additionally, the surface roughness and the interface roughness increase slightly due to a growing density gradient. After 34 d of storage the corrosion of the glass surface leads to a relatively thick sol-gel layer with a low density. The surface roughness increases drastically due to the corrosion products on the surface, which become visible by electron microscopy. The pronounced gradient in density makes it necessary to introduce an additional leached layer for the simulation to describe the measured data satisfactorily. This glass surface is no longer suitable for optical coatings. For certain coatings this is already valid for the surface after a storage of 11 d. Under ambient or dryer storage conditions this corrosion process also takes place but much slower.

#### 4. Conclusion

Grazing incidence X-ray reflectivity measurements give valuable information on the formation of surface layers which are evoked by very different processes. The fairly thin layers allow the distinction between the tin bath and the air side of the float glass which are caused by the production conditions. The spectra contain also information on the layer formation due to the interaction with air during a certain period of storing. In addition, the data allow to describe the quality of a polishing process on the basis of the roughness data. Hydration as well as leaching of glass components due to interaction with different environments can be studied.

The various information on the surfaces of glasses revealed by GIXR demonstrates that the technique is very surface-sensitive and provides data complementary to those yielded by other techniques. Moreover, since the method works in air (not in vacuum), investigations of volatile layers on glass are possible. This allows in-situ studies of different processes on glass surfaces in air.

#### 5. References

- [1] Hench, L. L.: Corrosion of silicate glasses. An overview. *Mater. Res. Soc. Symp. Proc.* **125** (1988) p. 189–200.
- [2] Bange, K.; Anderson, O.; Ottermann, C.: Coatings on glass. In: Bach, H. (ed.): *Schott series*. Vol. 4. Berlin (et al.): Springer, 1997.
- [3] Bange, K.; Anderson, O.; Ottermann, C. et al.: Stabilization of oxidic thin films. *BMFT Final Rep. FKZ 13N5476*. 1991.
- [4] Lengeler, B.; Campagna, M.; Rosei, K. (eds.): *X-ray absorption and reflection in the hard X-ray range. Photoemission and absorption spectroscopy of solids and interfaces with synchrotron radiation*. Amsterdam: North Holland, 1990.
- [5] James, R. W.: *The optical principles of the diffraction of X-rays*. Ithaca, NY: Cornell University Press, 1965. chap. 4.
- [6] Nénot, L.; Croce, P.: Caractérisation des surfaces par réflexion rasante de rayons X. Application à l'étude du polissage de quelques verres silicates. *Rev. Phys. Appl.* **15** (1980) no. 3, p. 761–779.
- [7] Lengeler, B.; Hüppauff, M.: Surface analysis by means of reflection, fluorescence and diffuse scattering of hard X-ray. *Fresenius J. Anal. Chem.* **346** (1993) p. 155–161.
- [8] Paratt, L. G.: *Phys. Rev.* **95** (1954), p. 359ff.
- [9] Press, W. H.; Teukolsky, S. A.: Simulated annealing optimization over continuous spaces. *Comput. Phys.* **4** (1991) p. 426–429.
- [10] Anderson, O.; Daalderop, G. H. O.; Bange, K.: X-ray reflectivity investigations of glass surfaces produced by float and draw techniques. *Mikrochim. Acta* (1997). (In press.)
- [11] Vigil, G.; Xu, Z.; Steinberg, S. et al.: Interaction of silica surfaces, *J. Colloid Interface Sci.* **165** (1994) p. 367–385.
- [12] Wagner, W.; Rauch, F.; Bach, H.: Chemical properties of hydrolyzed surface layers on  $\text{SiO}_2\text{-BaO-B}_2\text{O}_3$ . *Glastech. Ber.* **63** (1990) no. 12, p. 351–362.
- [13] Bach, H.; Großkopf, K.; March, P. et al.: In-depth analysis of elements and properties of hydrated subsurface layers on optical surfaces of a  $\text{SiO}_2\text{-BaO-B}_2\text{O}_3$  glass with SIMS, IBSCA, RBS and NRA. Pt. 1. Experimental procedures and results. Pt. 2. Discussion of results. *Glastech. Ber.* **60** (1987) no. 1, p. 21–30; no 2, p. 33–46.
- [14] Wagner, W.: Untersuchungen zur chemischen Beständigkeit von optischen Gläsern mit Methoden der Ionenstrahlanalyse. Diplomarbeit, Univ. Frankfurt/M. 1986.
- [15] Laube, M.: Einfluß der Umgebungsbedingungen auf die Elementverteilung in Floatglasoberflächen und Beschichtungen. Thesis, Univ. Frankfurt/M. 1996.
- [16] Grimal, J. M.; Chartier, P.; Lehuédé, P.: X-ray reflectivity: A new tool for the study of glass surfaces. *J. Non-Cryst. Solids* **196** (1996) p. 128–133.

■ 1097P005

Address of the authors:

O. Anderson, K. Bange  
Schott Glaswerke  
Servicebereich Forschung und Entwicklung  
Hattenbergstraße 10  
D-55122 Mainz